

Statistics of Spectra for One-dimensional Quasi-Periodic Systems at the Metal-Insulator Transition

Yoshihiro Takada,¹ Kazusumi Ino,¹ and Masanori Yamanaka²

¹*Department of Pure and Applied Sciences, University of Tokyo,
Komaba 3-8-1, Meguro-ku, Tokyo, 153-8902, Japan*

²*Department of Physics, College of Science and Technology, Nihon University,
Kanda-Surugadai 1-8, Chiyoda-ku, Tokyo, 101-8308, Japan*

We study spectral statistics of one-dimensional quasi-periodic systems at the metal-insulator transition. Several types of spectral statistics are observed at the critical points, lines, and region. On the critical lines, we find the bandwidth distribution $P_B(w)$ around the origin (in the tail) to have the form of $P_B(w) \sim w^\alpha$ ($P_B(w) \sim e^{-\beta w^\gamma}$) ($\alpha, \beta, \gamma > 0$), while in the critical region $P_B(w) \sim w^{-\alpha'}$ ($\alpha' > 0$). We also find the level spacing distribution to follow an inverse power law $P_G(s) \sim s^{-\delta}$ ($\delta > 0$).

PACS numbers: 05.45.Mt, 03.65.Sq, 71.30.+h, 71.23.An

The universality of statistical properties of energy spectrum is ubiquitously found in quantum physics [1], ranging from quantum chaos [2] to quantum chromodynamics [3]. In condensed matter physics, the metal-insulator (MI) transition in disordered electron systems gives a notable example of such universality. In the metallic side, the energy level statistics can be described by random matrix theory [4]. The level spacing distribution is close to the Wigner surmise. The universality class is classified by the symmetry of the system. In the insulating side the level spacing distribution is Poissonian. At the critical point, new statistical features emerge [5, 6]. They are different from random matrix theory and Poisson statistics. The universality of these new statistics dubbed as “critical level statistics” is also classified by symmetry of the ensemble [7, 8, 9, 10].

Quasi-periodic systems are other interesting ones showing the MI transition. The universality of the transition has been characterized by multifractal structures of bandwidths and wavefunctions (see Ref. [11] for a review). The Harper model [12, 13] is obtained by a gauge fixing of two-dimensional electrons on the square lattice in a uniform magnetic field. Especially incommensurate limits of the flux per plaquette, such as the inverse of the golden mean $\sigma = \frac{-1+\sqrt{5}}{2}$, have been extensively studied. In the atomic scale, the penetration of flux for each plaquette requires an enormous strength of magnetic field, but nowadays it is realized in laboratory on a quantum dot lattice [14].

The quasi-periodic system can be seen as a system between “periodic” and “random,” thus giving an interesting example of quantum “chaos.” Classically an open orbit (separatrix) of equi-energetic curve appears at the MI transition point. But the quantum transition cannot be understood by the classical consideration. It is not characterized by a single energy band corresponding to the separatrix but the wavefunctions for all the energy bands become critical with power-law decay. The energy

level statistics are different from disordered systems. It is not close to the Wigner surmise on the metallic side nor is the Poisson statistics seen on the insulating side [15]. Spectra of quasi-periodic systems have a fractal structure [12], which hinders established techniques used in disordered case such as “unfolding” to extract universal properties of fluctuations.

Recently Evangelou and Pichard [16] investigated the bandwidth distribution $P_B(w)$ (w : bandwidth) of the one-dimensional Harper model at the incommensurate limit of σ . They found that it agrees with the semi-Poisson statistics $P_B(w) = 4we^{-2w}$ with the sub-Poisson number variance $\Sigma_2(E) \sim \text{const.} + \chi E$ ($\chi < 1$) at the critical point. They argued that it is related to the universal characterization of quantum chaos.

Although this suggests that a characterization by level-statistical idea is possible for the MI transitions of a larger class of quasi-periodic systems, the universal appearance of the semi-Poisson statistics may be questioned from the experience in critical level statistics of disordered systems. In Ref.[7], it has been suggested the level spacing distribution may be described by a more generalized form $P(s) = As^\alpha e^{-\beta s^\gamma}$ ($\alpha, \beta, \gamma > 0$), and it has been observed in numerical studies [10]. A similar rich structure of critical level statistics should be expected for quasi-periodic systems.

Motivated by this idea, we investigate a generalization of the Harper model, namely the extended Harper model, which is obtained from two dimensional electrons on the square lattice with next-nearest-neighbor hopping in a uniform magnetic field [17, 18]. We find that such a rich structure indeed emerges for the critical level statistics of this extended model, but with some substantial modifications, even for the case treated in [16]. We explain this variety of critical level statistics by the quantum nature of the system.

Let us first describe the model. We consider the two-dimensional fermions on the square lattice in a flux per plaquette φ with next-nearest-neighbor coupling

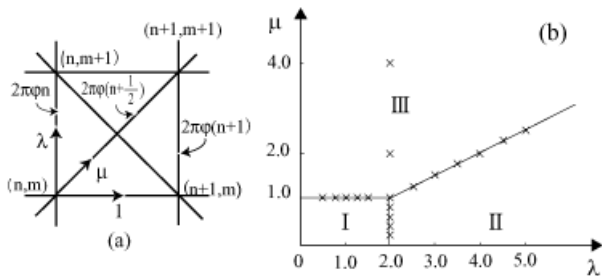


FIG. 1: (a) Transfer integrals of the extended Harper model (Eq.(1)) and (b) its phase diagram (See [17]). In region I the wavefunction (spectrum) is extended (absolutely continuous) and in region II it is localized (pure points). In region III and on the three boundary lines, it is critical (singular continuous).

(Fig.1(a)). The Hamiltonian is given by

$$H = \cos p_x + \lambda \cos x + \mu \cos(p_x + x) + \mu \cos(p_x - x), \quad (1)$$

where $p_x = -2\pi i \phi \frac{d}{dx}$. The positive parameters, λ and μ , are the strength of the kinetic terms for the perpendicular and next-nearest-neighbor directions respectively, while the horizontal one is normalized to unity. We take the Landau gauge $\Psi(x_n, y_n) = \psi_x(x_n) e^{i\nu y_n}$ and obtain the Schrödinger equation for $\psi_n = \psi_x(x_n)$ as

$$\begin{aligned} & \left[1 + \mu \cos \left(2\pi \left(n + \frac{1}{2} \right) \varphi + \nu \right) \right] \psi_{n+1} \\ & \quad + \lambda \cos(2\pi n \varphi + \nu) \psi_n \\ & + \left[1 + \mu \cos \left(2\pi \left(n - \frac{1}{2} \right) \varphi + \nu \right) \right] \psi_{n-1} = E \psi_n. \quad (2) \end{aligned}$$

At $\mu = 0$, this is reduced to the Harper model. For a rational $\varphi = p/q$ where p and q are relatively prime, Eq.(2) reduces to a $q \times q$ matrix with the boundary condition $\psi_{n+q} = \exp(ikq)\psi_n$, which can be transformed to be tridiagonal [18]. To investigate the irrational limit of $\varphi \rightarrow \sigma$, we use the rational approximation of $\varphi_j = F_{j-1}/F_j$ where F_j is the Fibonacci number satisfying $F_{j+1} = F_j + F_{j-1}$ with $F_0 = 1$ and $F_1 = 1$.

The phase diagram is shown in Fig.1(b). The scaling property of the bandwidth was studied in [17]. For large q , the minimum and maximum are obtained at either $k = 0$ or π/q for fixed ν [18]. We numerically diagonalized the matrices there setting $\nu = 0$ for simplicity, and obtained the bandwidth distribution $P_B(w)$. The normalizations are $\int_0^\infty P_B(w) dw = 1$ and $\langle w \rangle = \int_0^\infty w P_B(w) dw = 1$.

First, we study the bandwidth distribution along the critical line $\lambda = 2$. In Fig.2, we plot the $P_B(w)$ at $(\lambda, \mu) = (2.0, 0.4)$ for $j = 25, 27, 28$. It shows a good convergence to a limit distribution, indicating the existence of the limit of the bandwidth distribution at the incommensurate flux φ . For $0 \leq \mu < 1$, we find $P_B(w)$ exhibits a continuous change. It has been concluded [17]

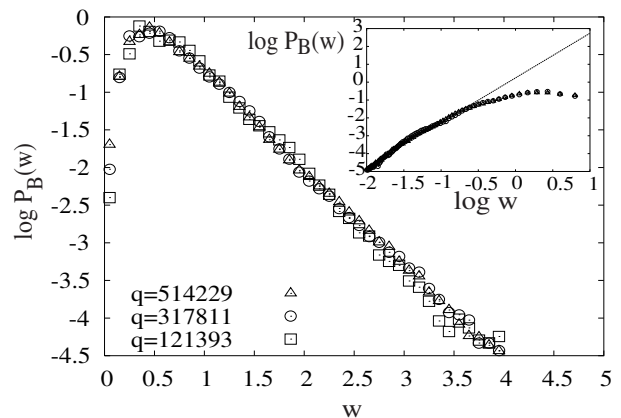


FIG. 2: The bandwidth distribution at $(\lambda, \mu) = (2.0, 0.4)$, and the one near the origin (inset).

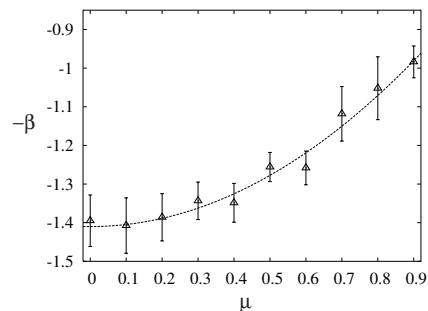


FIG. 3: μ -dependence of index β along the critical line $\lambda = 2$.

that the scaling property of the bandwidths is invariant on this line, implying the system belongs to the same universality class. The continuous change means that $P_B(w)$ is not a universal quantity.

In Fig.2, one sees linear behaviors at large w , implying an asymptotic form

$$P_B(w) \sim e^{-\beta w}, \quad \text{as } w \rightarrow \infty \quad (3)$$

where $\beta > 0$. The optimized values of β are shown in Table I. It suggests a quadratic dependence of β on μ . The best fit is attained by a quadratic function $\sim 1.4 - 0.53\mu^2$ (Fig.3). This rather simple dependence may be related to the universality class on this line.

$P_B(w)$ is estimated to be zero at the origin. Inset of Fig.2 shows $P_B(w)$ near the origin, indicating a power law. To characterize this behavior, we make an ansatz

$$P_B(w) \sim w^\alpha, \quad \text{as } w \rightarrow 0 \quad (4)$$

where $\alpha > 0$. The optimized values of $\alpha(\mu)$ are shown in Table I. One sees that $\alpha(\mu)$ s are stable, suggesting that $\alpha(\mu)$ is independent of μ at the incommensurate limit.

These numerical results suggest that the overall distribution is given by a generalized semi-Poisson form

$$P_B(w) = A w^\alpha e^{-\beta w} \quad (5)$$

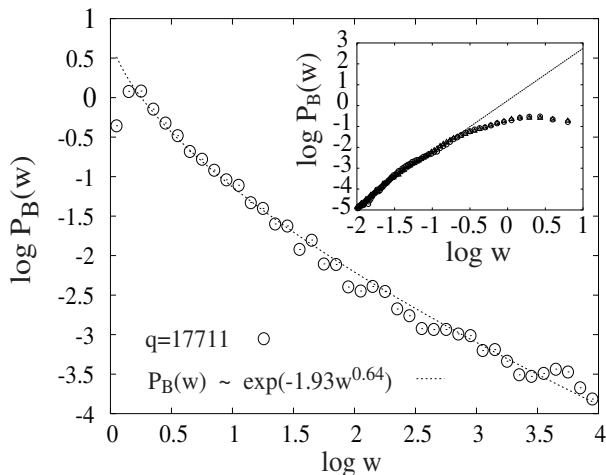


FIG. 4: The bandwidth distribution at $(\lambda, \mu) = (1.0, 1.0)$, and the one near the origin (inset).

where A is a normalization constant. The exact semi-Poisson form i.e. $\alpha = 1$, $\beta = 2$ has been reported at $(\lambda, \mu) = (2.0, 0.0)$ [16]. Actually the normalization conditions allow only one parameter α with $\beta = \alpha + 1$ and $A = \frac{(\alpha+1)^{\alpha+1}}{\Gamma(\alpha+1)}$. It is clear that such relations are not consistent with our results as shown in Table I. Especially the semi-Poisson statistics with $\alpha = 1$ do not reproduce the index of the power-law behavior around the origin at $\mu = 0$. Using one-parameter fit by (5), we get $\alpha \sim 0.7$ to the overall distribution, which is much smaller than that estimated by (4). For $\mu \neq 0$, we get similar deviations. Thus we may conclude that the semi-Poisson form for $P_B(w)$ is only an approximation to the overall distribution.

Next, we investigate $P_B(w)$ on the other critical lines. It turns out that the behaviors are different from those on the critical line $\lambda = 2$. Fig.4 shows the $P_B(w)$ at $(\lambda, \mu) = (1.0, 1.0)$. The large w behaviors do not show an exponential decay, but a milder one. Thus we make a generalized ansatz of

$$P_B(w) \sim e^{-\beta w^\gamma} \quad \text{as } w \rightarrow \infty \quad (6)$$

with $0 < \gamma < 1$. The optimized curve agrees well with the obtained data (Fig.4). The behavior near the origin is also found to follow a power law (inset of Fig.4). On the line $\mu = 1$, the index α seems to be constant around 1.5. We find that the numerical data on the critical line $\lambda = 2\mu$ can be also described by each ansatz (4) and (6). The index α is stable around 1.5 as in Table II, which is near the values on the critical line $\mu = 1$.

The overall distribution on the critical lines $\mu = 1$ and $\lambda = 2\mu$ except for the bicritical point may be cast in a form

$$P_B(w) = Aw^\alpha e^{-\beta w^\gamma}. \quad (7)$$

This form of distribution was suggested in Ref.[7] for the level spacing distribution of disordered systems at the MI transition. The $\gamma \neq 1$ case has been encountered in a 3D disordered system with orthogonal symmetry [10]. The normalization conditions constrain $\beta = \left(\frac{\Gamma(\frac{\alpha+2}{\gamma})}{\Gamma(\frac{\alpha+1}{\gamma})} \right)^\gamma$

and $A = \frac{\gamma \beta^{\frac{\alpha+1}{\gamma}}}{\Gamma(\frac{\alpha+1}{\gamma})}$. Our analysis does not support these constraints. Again, we tried a one-parameter fit varying $\alpha(\gamma)$ in (7) with the observed value of $\gamma(\alpha)$ fixed. We got values much smaller (larger) than the observed indices $\alpha(\gamma)$ around the origin (in the tail) for all the points we studied on the critical lines $\mu = 1$ and $\lambda = 2\mu$.

We also investigate the bicritical point at $(\lambda, \mu) = (2.0, 1.0)$. However, the convergence of the obtained distribution is slow, and we have not got information of the incommensurate limit.

The values of α and γ on the critical lines $\mu = 1$ and $\lambda = 2\mu$ are considerably smaller from those on $\lambda = 2$ ($\gamma=1$ there). This smallness of α and γ indicates the tendency of $P_B(w)$ on these critical lines to broaden both to the origin and the tail compared to $P_B(w)$ on $\lambda = 2$. This may imply that the transport property becomes different when μ gets sufficiently large. To supplement this observation, we investigate the bandwidth distribution in the critical region (the region III in Fig.1(b)). $P_B(w)$ follows an inverse power law $P_B(w) \sim w^{-\alpha'}$ ($\alpha' > 0$) there (Fig.5). The values of α' are summarized in Table I. This behavior sharply contrasts with the one seen on the critical lines. The divergence of $P_B(w)$ at the origin implies the dominance of relatively flat bands, indicating that in most of the bands the wavefunction is close to be localized. Also the power law decay in the tail means the appearance of bands whose wavefunction is close to be extended.

From the two-dimensional point of view, the next-nearest-neighbor hopping term (μ dependent term) is dominant in Eq.(1) in the critical region. Since y -translation is canonically conjugate to x -translation in the uniform magnetic field, the extension (localization) of the wavefunction in y -direction must be balanced by the localization (extension) in x -direction to satisfy the uncertainty principle. When μ is small, x -dependence of the wavefunction is determined by λ , the anisotropic parameter for y -direction. On the other hand, when μ is sufficiently large, as μ acts on x - and y -directions equally, the wavefunction is sensitive to μ by both of its x - and y -dependences. This makes the MI transition in the critical region different from that on the critical line $\lambda = 2$, resulting in the increase of the bands close to be localized as well as the bands close to be extended. Thus the appearance of the inverse power law in the critical region and the differences of α and γ among the critical lines are consequences of quantum nature of the system.

We also investigate the gap distribution $P_G(s)$. The gap distribution at $(\lambda, \mu) = (2.0, 0.0)$ has been known to

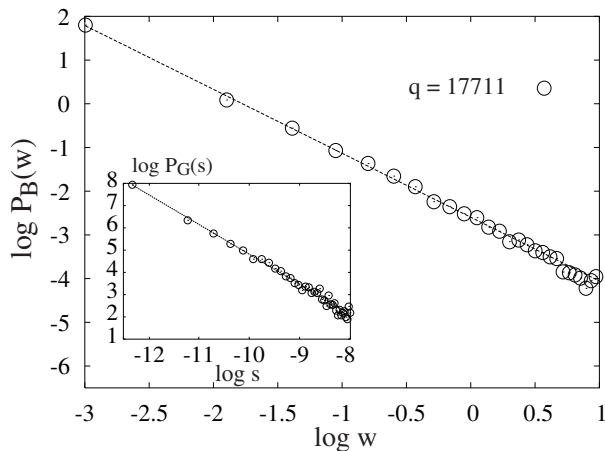


FIG. 5: The band width distribution and level spacing distribution (inset) at $(\lambda, \mu) = (2.0, 2.0)$.

follow an inverse power law [19, 20], which diverges at the origin

$$P_G(s) \sim s^{-\delta} \quad (8)$$

with $\delta \sim 1.5$. We find $P_G(s)$ along the three critical lines and in the critical region also follows an inverse power law (inset of Fig.5). The values of δ are shown in Table I and II.

It would be interesting to examine a similar statistical distribution for the wavefunctions. The characterization through level-statistical idea may have a good possibility.

In this letter, we have seen that a systematic characterization by a level-statistical idea for the quasi-periodic system is possible. We have investigated the bandwidth $P_B(w)$ and gap distributions $P_G(s)$ for one-dimensional quasi-periodic Schrödinger equations at the MI transition and confirmed their variety as expected. We found a power law $P_B(w) \sim w^\alpha$ near the origin and a generalized exponential decay $P_B(w) \sim e^{-\beta w^\gamma}$ ($\alpha, \beta, \gamma > 0$) on the critical lines, while in the critical region $P_B(w)$ follows an inverse power law $\sim w^{-\alpha'}$ ($\alpha' > 0$). We gave the explanation for this variety of $P_B(w)$ by quantum nature of the system. A surmise of a form $P_B(w) = Aw^\alpha e^{-\beta w^\gamma}$ gives only an approximation. The gap distribution $P_G(s)$ shows an inverse power law $\sim s^{-\delta}$ for whole the phase diagram. For the bicritical point, we did not get a conclusive result.

Acknowledgments Y.T. and K.I. thank S. Hikami for useful discussions. K.I. thanks A. Garcia-Garcia for discussion and M. Kohmoto for explaining previous results. K.I. has benefited from the Grand-in-Aid for Science(B), No.1430114 of JSPS.

λ	μ	α	β	δ
2.0	0.0	2.5(± 0.1)	1.39(± 0.07)	1.5(± 0.2)
2.0	0.1	2.5(± 0.1)	1.41(± 0.07)	1.5(± 0.2)
2.0	0.2	2.5(± 0.1)	1.39(± 0.06)	1.5(± 0.2)
2.0	0.3	2.51(± 0.08)	1.34(± 0.05)	1.5(± 0.1)
2.0	0.4	2.51(± 0.08)	1.35(± 0.05)	1.5(± 0.2)
2.0	0.5	2.50(± 0.06)	1.26(± 0.04)	1.5(± 0.2)
2.0	0.6	2.52(± 0.07)	1.26(± 0.04)	1.5(± 0.2)
2.0	0.7	2.54(± 0.07)	1.12(± 0.07)	1.5(± 0.2)
2.0	0.8	2.52(± 0.07)	1.05(± 0.08)	1.5(± 0.1)
2.0	0.9	2.48(± 0.04)	0.98(± 0.11)	1.47(± 0.04)
2.0	1.0	-	-	1.2(± 0.3)
2.0	2.0	-1.46(± 0.06)	-	1.34(± 0.07)
2.0	4.0	-1.5(± 0.1)	-	1.1(± 0.1)
2.0	6.0	-1.37(± 0.08)	-	1.3(± 0.2)

TABLE I: The optimized indices on the critical line $\lambda = 2$ and in the critical region. For the definitions of α , β , and δ , see Eqs.(3), (4), and (8) respectively. Also the value of α in the critical region is defined as $-\alpha'$.

λ	μ	α	γ	δ
0.5	1.0	1.55(± 0.14)	0.41(± 0.04)	1.29(± 0.08)
0.75	1.0	1.48(± 0.17)	0.52(± 0.08)	1.3(± 0.2)
1.0	1.0	1.48(± 0.12)	0.65(± 0.07)	1.3(± 0.2)
1.25	1.0	1.61(± 0.17)	0.53(± 0.05)	1.4(± 0.2)
1.5	1.0	1.48(± 0.13)	0.60(± 0.07)	1.29(± 0.10)
2.5	1.25	1.44(± 0.10)	0.54(± 0.06)	1.31(± 0.10)
3.0	1.5	1.61(± 0.13)	0.51(± 0.04)	1.3(± 0.2)
3.5	1.75	1.49(± 0.14)	0.38(± 0.04)	1.5(± 0.2)
4.0	2.0	1.43(± 0.13)	0.60(± 0.06)	1.3(± 0.2)
4.5	2.25	1.64(± 0.15)	0.64(± 0.03)	1.3(± 0.3)
5.0	2.5	1.34(± 0.19)	0.50(± 0.04)	1.4(± 0.2)

TABLE II: The optimized indices for the bandwidth distribution and level spacing distribution on the critical lines of $\mu = 1$ and $\lambda = 2\mu$. For the definition of γ , see Eq.(6).

[1] See, for example, T. Guhr, A. Müller-Groeling, and H. A. Weidenmüller, Phys. Rep. **299**, 189 (1998).

- [2] O. Bohigas, in Chaos and Quantum Physics, Proceedings of the Les Houches Summer School, edited by M. J. Giannoni, A. Voros, and J. Zinn-Justin (Elsevier, New York, 1991).
- [3] J. Verbaarschot, Nucl. Phys. B (Proc. Suppl.) **53**, 88 (1997).
- [4] E.P. Wigner, Proc. Camb. Philos. Soc. **47**, 790 (1951); F.J. Dyson, J. Math. Phys. **3**, 140 (1962); *ibid.* 157 (1962); *ibid.* 166 (1962).
- [5] B.L. Altshuler, I.Kh. Zharekeshv, S.A. Kotochigova and B.I. Shklovskii, Sov. Phys. JETP **67**, 625 (1988).
- [6] B.I. Shklovskii, B. Shapiro, B.R. Sears, P. Lambrianides, and H.B. Shore, Phys. Rev. B **47**, 11487 (1993).
- [7] A.G. Aronov, V.E. Kravtsov, and I.V. Lerner, JETP Lett. **59**, 39 (1994); Phys. Rev. Lett. **74**, 1174 (1995).
- [8] T. Kawarabayashi, T. Ohtsuki, K. Slevin, and Y. Ono, Phys. Rev. Lett. **77**, 3593 (1996).
- [9] E. Cuevas, Phys. Rev. Lett. **83**, 140 (1999).

- [10] E. Hofstetter and M. Schreiber, Phys. Rev. B **48**, 16979 (1993); *ibid.* **49**, 14726 (1994).
- [11] H. Hiramoto and M. Kohmoto, Int. J. Mod. Phys. **B 6** 281(1992).
- [12] M.Ya. Azbel, Zh. Eksp. Teor. Fiz. **46**, 929 (1964); D.R. Hofstadter, Phys. Rev. B **14**, 2239 (1976).
- [13] S. Aubry and G. André, Ann. Israel Phys. Soc. **3**, 133 (1980).
- [14] C. Albrecht, J.H. Smet, K.von Klitzing, D. Weiss, V. Umansky, and H. Schweizer, Phys. Rev. Lett. **86**, 147 (2001).
- [15] A.P. Megann and T. Ziman, J. Phys. **A 20**, L1257 (1987).
- [16] N. Evangelou and J.-L. Pichard, Phys. Rev. Lett. **84**, 1643 (2000).
- [17] J.H. Han, D.J. Thouless, H. Hiramoto, and M. Kohmoto, Phys. Rev. B **50**, 11365 (1994).
- [18] D.J. Thouless, Phys. Rev. B **28**, 4272 (1983); D.J. Thouless, Commun. Math. Phys. **127**, 187 (1990).
- [19] K. Machida and M. Fujita, Phys. Rev. B **34**, 7367 (1986).
- [20] T. Geisel, R. Ketzmerick, and G. Petschel, Phys. Rev. Lett. **66**, 1651 (1991).